




Role of Estrogen-Related Receptor γ and PGC-1 α /SIRT3 Pathway in Early Brain Injury After Subarachnoid Hemorrhage

Yong Guo^{1,2} · Yongmei Hu^{2,3} · Yi Huang^{2,4} · Lei Huang^{2,5} · Hideki Kanamaru² · Yushin Takemoto² · Hao Li¹ · Dujuan Li² · Jianjun Gu¹ · John H. Zhang^{2,5} 

Accepted: 30 October 2022 / Published online: 8 December 2022

© The American Society for Experimental Neurotherapeutics, Inc. 2022, corrected publication 2023

Abstract

Estrogen-related receptors (ERRs) were shown to play an important role in the regulation of free radical-mediated pathology. This study aimed to investigate the neuroprotective effect of ERR γ activation against early brain injury (EBI) after subarachnoid hemorrhage (SAH) and the potential underlying mechanisms. In a rat model of SAH, the time course of ERRs and SIRT3 and the effects of ERR γ activation were investigated. ERR γ agonist DY131, selective inhibitor GSK5182, or SIRT3 selective inhibitor 3-TYP were administered intracerebroventricularly (icv) in the rat model of SAH. The use of 3-TYP was for validating SIRT3 as the downstream signaling of ERR γ activation. Post-SAH assessments included SAH grade, neurological score, Western blot, Nissl staining, and immunofluorescence staining in rats. In an *in vitro* study, the ERR γ agonist DY131 and ERR γ siRNA were administered to primary cortical neurons stimulated by Hb, after which cell viability and neuronal deaths were accessed. Lastly, the brain ERR γ levels and neuronal death were accessed in SAH patients. We found that brain ERR γ expressions were significantly increased, but the expression of SIRT3 dramatically decreased after SAH in rats. In the brains of SAH rats, ERR γ was expressed primarily in neurons, astrocytes, and microglia. The activation of ERR γ with DY131 significantly improved the short-term and long-term neurological deficits, accompanied by reductions in oxidative stress and neuronal apoptosis at 24 h after SAH in rats. DY131 treatment significantly increased the expressions of PGC-1 α , SIRT3, and Bcl-2 while downregulating the expressions of 4-HNE and Bax. ERR γ antagonist GSK5182 and SIRT3 inhibitor 3-TYP abolished the neuroprotective effects of ERR γ activation in the SAH rats. An *in vitro* study showed that Hb stimulation significantly increased intracellular oxidative stress in primary cortical neurons, and DY131 reduced such elevations. Primary cortical neurons transfected with the ERR γ siRNA exhibited notable apoptosis and abolished the protective effect of DY131. The examination of SAH patients' brain samples revealed increases in ERR γ expressions and neuronal apoptosis marker CC3. We concluded that ERR γ activation with DY131 ameliorated oxidative stress and neuronal apoptosis after the experimental SAH. The effects were, at least in part, through the ERR γ /PGC-1 α /SIRT3 signaling pathway. ERR γ may serve as a novel therapeutic target to ameliorate EBI after SAH.

Keywords Estrogen-related receptors · Oxidative stress · Apoptosis · Neuroprotection · Subarachnoid hemorrhage

Yong Guo, Yongmei Hu, and Yi Huang contributed equally to this work.

✉ Jianjun Gu
gujianjundt@163.com

✉ John H. Zhang
johnzhang3910@yahoo.com

¹ Department of Neurosurgery, Henan Provincial People's Hospital, (People's Hospital of Zhengzhou University), Zhengzhou 450003, China

² Department of Physiology and Pharmacology, Loma Linda University, Loma Linda, CA 92350, USA

³ Department of Nursing, Henan Provincial People's Hospital, (People's Hospital of Zhengzhou University), Zhengzhou, Henan 450003, China

⁴ Department of Neurosurgery, Ningbo Hospital, Zhejiang University School of Medicine, Ningbo, Zhejiang 315010, China

⁵ Department of Neurosurgery, Loma Linda University, Loma Linda, CA 92350, USA

Introduction

Subarachnoid hemorrhage (SAH) is a devastating form of cerebrovascular disease that leads to high mortality and disability [1, 2]. Early brain injury (EBI) occurring within 72 h has been proposed to be a major cause of poor outcomes in SAH patients [3]. The mitochondria-mediated oxidative stress and neuronal apoptosis play crucial roles in this pathological process [4, 5]. Thus, neuroprotective strategies against oxidative stress and apoptosis specifically would be of the most clinical significance for attenuating EBI in SAH patients.

There is an imbalance between the reactive oxygen species (ROS) and the intrinsic antioxidant systems in the brain after SAH. Mitochondria have been considered the main source of ROS due to an ischemic disruption of the electron transfer chain following SAH [6, 7]. Recently, increasing evidence has indicated that the estrogen-related receptors (ERRs), a sub-class of nuclear receptors, play an important role in the regulation of ROS pathophysiology [8, 9]. It was reported that ERR α and ERR γ regulated the promoters of genes encoding tricarboxylic acid (TCA) cycle proteins and oxidative phosphorylation (OXPHOS) machinery [10, 11]. Meanwhile, the ERRs have been found to bind to regulatory regions of genes encoding the vast majority of the components of antioxidant defense systems, including superoxide dismutase (SODs) and peroxiredoxins (PRXs) [12]. The ERRs directly target and regulate SOD2, which codes for MnSOD [8] and SOD1 in different tissues and cell lines. Moreover, ERR α regulates SIRT3, which in turn increases the expression of the ROS-detoxifying enzyme SOD2 to decrease ROS levels [13]. Further evidence supports that the ERRs not only target these genes but also modulate their coactivator peroxisome proliferator-activated receptor coactivator-1 (PGC-1 α) [14]. In fact, PGC-1 α upregulation increases the levels of MnSOD/SOD2, PRX3/5, and UCP2) and also promotes cell survival by protecting cancer cells from the excessive mitochondrial ROS generation [15, 16]. In general, the ERRs possess the ability to regulate all the mitochondrial ROS production at the transcriptional level, including the TCA cycle, electron-transport chain (ETC) complexes I, II, and III, as well as a large number of ROS-generating enzymes [12].

Despite research indicating that ERRs are widely expressed in the central nervous system [17], there have been few studies on ERRs in stroke and none on their expression in the human brain. An interesting study reports that the neuronal ERR γ ablation decreases metabolic capacity in the hippocampus and impairs spatial learning and memory formation in mice [18]. DY131 is an agonist that can induce the transcriptional activity of ERR γ and regulate ERR γ -mediated metabolism [19, 20]. In animal models of

acute liver injury, DY131 treatment attenuated the lipopolysaccharide (LPS)-induced production of hepatocytic ROS by increasing the expression of SODs and ROS clearance [21]. However, the effects of ERR γ activation in EBI after SAH have never been reported.

In the current study, we hypothesized that ERRs would play an important role in EBI after SAH. The time course of ERRs changes in the brain of SAH rats and the effects of ERR γ agonist DY131 and ERR γ /PGC-1 α /SIRT3 signaling pathway against the oxidative stress injury and neuronal apoptosis were evaluated after experimental SAH in rats and in primary cultured neuronal cells.

Materials and Methods

Ethics Statement

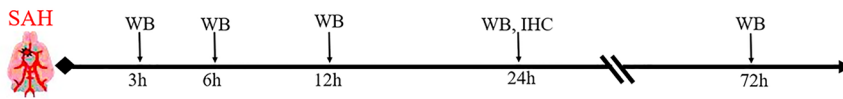
All animal procedures were approved by the Institutional Animal Care and Use Committee (IACUC) of Loma Linda University and were performed in accordance with the National Institutes of Health Guidelines for the Use of Animals in Neuroscience Research and the ARRIVE guidelines (Animal Research: Reporting of In Vivo Experiments). This human study was conducted in compliance with the guidelines of the Declaration of Helsinki and approved by the Human Ethics Committee of Henan Provincial People's Hospital, Zhengzhou, China. All of the patients in this study provided signed informed consent.

Animal Study

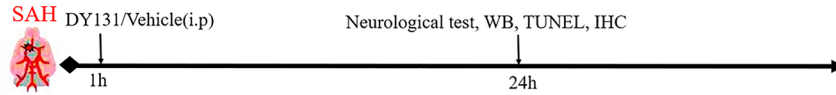
Study Design

Animals and Study Design Adult male Sprague–Dawley (SD) rats (age, approximately 2 months; weight, 280–320 g) were purchased from Harlan Laboratories (Indianapolis, Indiana) and housed in the Animal Care Facility of LLU with a 12-h light/dark cycle. Four separate experiments were performed in this study (Fig. 1). Rats were randomly assigned to each experimental group. The excluded rats (those that died during surgery or mild SAH grading) were replaced to ensure the same number of rats/group for statistical analysis.

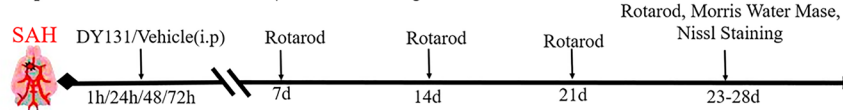
Experiment 1 To study the temporal expression and cellular localization of ERRs, 36 rats were randomly assigned to six groups: Sham ($n=6$), SAH-3 h ($n=6$), SAH-6 h ($n=6$), SAH-12 h ($n=6$), SAH-24 h ($n=6$), and SAH-72 h ($n=6$). Western blot analysis was performed to determine

Experiment 1: Time-course and Cellular Localization of $ERR\alpha$, $ERR\beta$, $ERR\gamma$ and SIRT3**Exper. 1 Groups:**

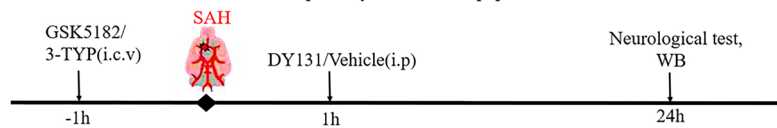
1. Sham (n=8)
2. SAH+3 h (n=6)
3. SAH+6 h (n=6)
4. SAH+12 h (n=6)
5. SAH+24 h (n=8)
6. SAH+72 h (n=6)

Experiment 2: The effects of $ERR\gamma$ activation on short-term neurobehavior, oxidative stress and neuronal apoptosis**Exper.2 Groups:**

1. Sham (n=10)
2. SAH+Vehicle (n=10)
3. SAH+DY131(2mg/kg) (n=6)
4. SAH+ DY131(6mg/kg)* (n=10)
5. SAH+ DY131(18mg/kg) (n=6)

Experiment 3: The effects of $ERR\gamma$ activation on long-term neurobehavioral outcome**Exper.3 Groups:**

1. Sham (n=10)
2. SAH+Vehicle (n=10)
3. SAH+DY131 (n=10)

Experiment 4: The effects of PGC-1 α /SIRT3 pathway on neuronal apoptosis and oxidative stress after SAH**Exper.4 Groups:**

1. Sham (n=6)
2. SAH + Vehicle (n=6)
3. SAH + DY131 (n=6)
4. SAH + DY131 + DMSO (n=6)
5. SAH + DY131 + GSK5182 (n=6)
6. SAH + DY131 + 3-TYP (n=6)

Fig. 1 Experimental design and animal groups

the expressions of ERRs in the ipsilateral (left) brain hemisphere. An additional 4 rats in the Sham ($n=2$) and SAH-24 h ($n=2$) groups were used for double immunofluorescence staining of cellular localization.

Experiment 2 To evaluate the effects of selective $ERR\gamma$ agonist DY131 on short-term outcomes after SAH, 42 rats were randomly assigned to five groups: Sham ($n=10$), SAH+Vehicle (10% DMSO, $n=10$), SAH+DY131 (2 mg/kg, $n=6$), SAH+DY131 (6 mg/kg, $n=10$), and SAH+DY131 (18 mg/kg, $n=6$). The selective $ERR\gamma$ agonist DY131 was administered by intracerebroventricular (icv) injection 1 h after SAH. SAH grade and neurological deficiency were assessed at 24 h after SAH. Based on the results of neurological tests, DY131 (6 mg/kg) was used as the optimal dose for further evaluating brain oxidative stress and neuronal apoptosis by Western blot, TUNEL, and Mitosox staining.

Experiment 3 To evaluate the effects of DY131 on long-term outcomes after SAH, 30 rats were randomly assigned into three groups ($n=10$ /group): Sham, SAH+Vehicle, and SAH+DY-131 (6 mg/kg). Rotarod test was performed on day 7, day 14, and day 21 after SAH. Morris water maze was performed on days 22–27 after SAH. The rats were euthanized on day 28 to assess the neuronal degeneration using Nissl staining.

Experiment 4 To explore the potential mechanism of $ERR\gamma$ /PGC-1 α /SIRT3 underlying DY131 treatment-mediated

neuroprotective effects after SAH, the selective $ERR\gamma$ inhibitor GSK5182 or selective SIRT3 antagonist 3-TYP was administered by icv injection 1 h before SAH. In addition to the shared brain samples from the Sham groups from Experiment 2, an additional 30 rats were randomly assigned into 5 groups ($n=6$ /group): SAH+Vehicle, SAH+DY131, SAH+DY131+DMSO, SAH+DY131+GSK5182, and SAH+DY131+3-TYP. Western blots were performed at 24 h after SAH.

SAH Model

The endovascular perforation model of SAH was performed as previously described [23]. Briefly, isoflurane-anesthetized (4% induction, 2.5% maintenance) rats were intubated and connected to the ventilator in the supine position. After exposing the left common carotid artery (CCA), external carotid artery (ECA), and internal carotid artery (ICA), the ECA was ligated and fashioned into a stump. The suture was advanced into ICA from the ECA stump through the common carotid bifurcation. The suture was advanced further into the intracranial ICA until resistance was felt (15 to 18 mm from the common carotid bifurcation) and then pushed another 3 mm to perforate the ICA wall before being withdrawn. Rats in the Sham group underwent the same procedures, except for blood vessel wall puncture. All animals were monitored intraoperatively, in which the heart rate, respiration, skin color, and pedal reflex were assessed intraoperatively every 5 min to

confirm the anesthetic status and prevent distress. After the completion of surgery and weaning from ventilation, the animals were transferred into a heated chamber, maintained at a temperature of 37.5 °C, for recovery. Respiration, heart rate, and skin color were monitored postoperatively every 15 min until normal behavior resumed.

The SAH grade was evaluated by an investigator who was blind to the experiment groups through a grading system immediately after euthanasia, as previously described [23]. The animals received a total score ranging from 0 to 18 after adding the scores from all six segments. SAH rats with a score of 8 or less were excluded from this study.

Treatment Administration

Two administration routes were used, including the icv route and the intraperitoneal (ip) route.

Selective EER γ agonist DY131 (TOCRIS, Minneapolis, MN, USA) was dissolved in dimethyl sulfoxide (DMSO) and further diluted with saline, then administered via ip injection at three different dosages (2, 6, or 18 mg/kg) 1 h after SAH according to the previous study [24]. For the long-term outcome study, an additional dose of DY131 was injected on days 2 and 3 after SAH. The drugs, including GSK5182 (ERR γ selective inhibitor, 12 μ mol/ml) and 3-TYP (SIRT3 selective inhibitor, 40 μ mol/ml), were dissolved in 1% dimethyl sulfoxide (DMSO) with a total volume of 5 μ l and administered via icv injection 1 h before surgery.

The icv injection was performed, as previously described [25]. Rats were placed in a stereotaxic apparatus under 2.5% isoflurane anesthesia. A precision 10- μ l syringe (Hamilton Company, Reno, NV) was inserted through a burr hole into the left lateral ventricle (0.9 mm caudal and 1.5 mm lateral to the bregma, 3.3 mm below the horizontal plane of the skull). Drugs were infused at a rate of 1 μ l/min to prevent possible leakage, and the needle was removed at 5 min after icv infusion completion. Lastly, the skull hole was sealed quickly with bone wax, and the incision site was sutured.

In Vitro Study

To evaluate the effects of DY131 against hemoglobin (Hb)-induced neuronal toxicity in vitro, primary cultured cortical neurons were randomly divided into 5 groups: the Sham group, Hb+ Vehicle group, Hb+DY131 group, Hb+DY131+ERR γ ScrRNA group, and Hb+DY131+ERR γ siRNA group. Replicates of four were performed for each group. Primary cultured cortical neurons were incubated with Hb and DY131 for various periods (24, 48, or 72 h). ERR γ siRNA was used for ERR γ knockdown in vitro. The neurons were

collected for Western blot analysis and immunofluorescence staining.

Primary Culture of Rat Cortical Neurons

Cortical neurons were cultured using a modified method reported by Redmond et al. [26]. Briefly, whole brains were removed aseptically from 1-day-old rat pups, and cortical tissues were dissected out. After removing the blood vessels and meninges, the tissues were incubated with 0.05% trypsin for 10 min at 37 °C, neutralized, and triturated by a Pasteur pipette. Huge particles were eliminated before neurons were seeded on poly-L-lysine-precoated plates with DMEM/F12 containing 10% fetal bovine serum (FBS, Gibco, Bethesda, MD, USA) at a density of 5×10^4 cells/ml and cultivated in a humidified atmosphere of 95% air/5% CO₂ at 37 °C. After cell attachment, the medium was changed to a neurobasal medium (Gibco, MD, USA) containing 2% B₂₇ (Gibco) and 0.5 mM glutamine, and then the medium was changed every 3 days. Arabinosylcytosine (5 μ g/ml) was added on the third day after incubation to prevent the growth of non-neuronal cells. Cells were used for experiments on the seventh day of culture.

siRNA Transfection in Cell Culture

Prior to transfection, primary cortical neurons were allowed to reach 80% confluence in poly D-lysine-coated 24-well plates. Scramble siRNA (Thermo Fisher Scientific, Waltham, MA, USA) and EER γ siRNA (Thermo Fisher Scientific, Waltham, MA) were prepared according to the manufacturer's protocol. Briefly, a stock of 10 μ M siRNA was prepared, and 4 μ l of this stock was mixed with 125 μ l Opti-MEM. In a separate tube, 7 μ l Lipofectamine 3000 was mixed with 125 μ l Opti-MEM. The two tubes were combined and left to sit at room temperature for 15–45 min; 250 μ l mixture/well was applied to cells, and an additional 1 ml Opti-MEM was added. After being transfected for 24 h, the transfected neurons were exposed to Hb and treated with DY131, as described above. Thereafter, cell viability, TUNEL, Mitosox, and Western blot of EER γ were also accessed.

Cell Viability Assay

Cell viability was determined by counting the number of adherent cells. The counting method was performed as previously described [27]. Cells were seeded at a density of 5×10^4 cells per well in 24-well plates. After 2 days, the cells were preincubated with EER γ agonist DY131 or saline for 30 min at 37 °C before the final addition of Hb (0.3 mg/ml). The cells with EER γ agonist and Hb were incubated for various periods (24, 48, or 72 h). After incubation, nonadherent cells were removed by 2 washes with PBS. Adherent cells were harvested by trypsinization, and trypan blue (0.04 g/dl) was added for 10 min. The number

of cells was counted in a hemocytometer. Cell viability was expressed as a percentage of the viable cells in experimental wells compared with that in wells of saline control.

Human Study

Clinical Sample Collection and Analysis

Patients with aneurysmal SAH are diagnosed by computerized tomography (CT) and digital subtraction angiography (DSA). Patients with a history of central nervous system (CNS) disease (e.g., CNS infection, stroke, traumatic brain injury, and spinal cord injury) or other organ dysfunctions within 6 months were excluded from the study.

The brain samples were obtained from SAH patients (6 male patients at an average age of 51.83 ± 6.68 years old) who received intracranial aneurysm clipping using a pterional approach in 3 days after SAH from 1 January 2020 to 1 January 2021 at Henan Provincial People's Hospital, Zhengzhou, China (Fig. 8A, B). Age- and sex-matched patients with drug-resistant epilepsy (6 male patients at an average age of 48.67 ± 11.48 years old) who received temporal lobectomy were also selected from the Henan Provincial People's Hospital as controls. Body weight and height were recorded for subsequent calculation of body mass index (BMI) using a standard formula: $\text{BMI (kg/m}^2\text{)} = \text{body weight (kg)}/\text{height (m}^2\text{)}$. SAH severity was assessed using the Hunt–Hess grades (Fig. 8A, B). The brain tissue sample was processed for Western blot assay and IHC staining. Equal amounts of protein samples were separated by SDS-PAGE gel and transferred to a nitrocellulose membrane. The membranes were blocked and incubated overnight at 4 °C with the following primary antibodies: anti-ERR γ (1:1000, LSBio, USA) and anti-cleaved caspase-3 (1:1000, Cell Signaling Technology, MA, USA). Appropriate secondary antibodies (1:5000, Bioworld Technology) were incubated at room temperature for 2 h. The specific bands were visualized by an ECL reagent (Amersham Biosciences, Pittsburgh, PA, USA). The relative densities of the immunoblot bands were analyzed using ImageJ software (ImageJ 1.4, NIH, USA). The team blinded to the clinical parameters of the patients performed the Western blot analysis. IHC was performed as previously described [22]. For primary antibodies, we used anti-ERR γ (1:200, LSBio, USA) and anti-cleaved caspase-3 (1:200, Cell Signaling Technology, MA, USA). The staining positive cells were observed and imaged under a light microscope by an investigator blinded to the groupings, and the mean percentage of positive cells was averaged from the six randomly selected regions in each coronary section under a magnification of $\times 200$ for final analysis.

Behavioral Analysis

Short-term Neurological Evaluation

The short-term neurobehavioral performance was evaluated at 24 h after SAH by an investigator blind to the experiment groups. The 18-point modified Garcia score and 4-point beam balance test were used as previously described [25]. Higher scores indicated better neurological performance.

Long-term Neurological Evaluation

Rotarod Test The rotarod test was performed to evaluate sensorimotor coordination and balance on days 7, 14, and 21 after SAH, as previously described [25]. The rotating speed began at 5 revolutions per minute (RPM), or 10 RPM, and was gradually increased by 2 RPM every 5 s. The duration that rats were able to stay on the accelerating rotating cylinder was recorded by a photo beam circuit.

Morris Water Maze The Morris water maze test was started on days 22–27 after SAH to evaluate spatial learning capacity and memory ability, as previously shown [28]. Briefly, the animal was taken to the platform and kept there for 5 s on the first day of cueing test. During the following days of the spatial learning test, animals were released in a semi-random set of starting positions and were tasked with finding the submerged platform. The time limit for each animal to find the platform was 60 s. The probe test was performed on day 27 after SAH, in which animals were allowed to search for platform areas after removing the actual platform. A video recording system traced the activities of the animals, and the swim patterns were measured for quantification of distance, latency, and swimming speed by Video Tracking System SMART-2000 (San Diego Instruments Inc., CA, USA).

Western Blot and Immunoprecipitation

The total protein and surface membrane protein samples were extracted from the brain tissues of rats or primary cultured neurons for immunoblotting analysis. Western blotting was performed as described previously [29]. Briefly, the samples of ipsilateral brain hemisphere or primary cortical neurons collected 48 h after Hb treatment were extracted in RIPA buffer (Santa Cruz Biotechnology, CA, USA) and centrifuged with $14,000 \times g$ at 4 °C for 30 min. The supernatant was collected, and the protein concentration measurement was measured using a detergent-compatible assay (DC protein assay, Bio-Rad Laboratories, CA, USA). Equal amounts of protein samples were

separated by SDS-PAGE gel and transferred to a nitrocellulose membrane. The membranes were blocked and incubated overnight at 4 °C with the following primary antibodies: anti-ERR α (1:1000, PPMX, Tokyo, Japan), anti-ERR β (1:1000, PPMX, Tokyo, Japan), anti-ERR γ (1:1000, LSBio, USA), anti-PGC-1 α (1:1000; Abcam, Cambridge, MA, USA), anti-SIRT3 (1:1000; Cell signaling, USA), anti-Ac-SOD/SOD (1:1000 Abcam, Cambridge, MA, USA), anti-4-HNE (1:1000, ab46545, Abcam, MA, USA), anti-Bcl-2 (1:1000, ab59348, Abcam, MA, USA), anti-Bax (1:4000, ab182734, Abcam, MA, USA), and anti- β -actin (1:5000, sc-47778, Santa Cruz Biotechnology, TX, USA). Appropriate secondary antibodies (1:3000, Santa Cruz, Dallas, TX, USA) were incubated at room temperature for 2 h. The specific bands were visualized by an ECL reagent (Amersham Biosciences, Pittsburgh, PA, USA). The relative densities of the immunoblot bands were analyzed using ImageJ software (ImageJ 1.4, NIH, USA).

Coimmunoprecipitation (Co-IP) was performed to detect the protein interaction between ERR γ and PGC-1 α . Briefly, protein A/G Sepharose beads (50 μ l, ab193262, Abcam, MA, USA) were added into the protein lysate (200 μ l) and incubated with 5 μ g anti-ERR γ (PPMX, Tokyo, Japan) or normal mouse IgG (Santa Cruz, TX, USA) at 4 °C overnight. The beads were gently rinsed with PBS (precold, 0.01 M) and collected after centrifugation at 14,000 rpm at 4 °C for 30 min. The beads were resuspended in 200 μ l loading buffer and heated at 95 °C for 10 min. The Western blot assessments and data analysis were subsequently performed as described above.

Histology

Immunofluorescence Staining

Brain slices (10 μ m thick) were washed three times in 0.01 M of PBS for 5 min and incubated in 0.3% Triton X-100 in 0.01 M of PBS for 5 min at room temperature, after which the slices were further blocked with 5% donkey serum in 0.01 M of PBS for 1 h at room temperature. Primary cortical neurons were cultured in a glass-bottomed vessel for 30 min at 37 °C, protected from light, washed with PBS, fixed in 4% PFA for 30 min at room temperature, and permeated for 10 min with 0.1% Triton X-100 in PBS. The cells were then washed with PBS and blocked with 1% BSA for 1 h at 37 °C. Brain slices or fixed cells were incubated at 4 °C overnight with primary antibodies including anti-ERR γ (1:200, LS-A5960, LSBio, USA) and anti-NeuN (1:500, ab177487, Abcam, Cambridge, MA, USA). On the second day, the brain slices were washed with 0.01 M of PBS and incubated

with fluorescence-conjugated secondary antibodies (1:500, Jackson ImmunoResearch, PA, USA) for 1 h at room temperature. The nuclei were stained using a DAPI solution for 5 min at room temperature, and the cells were subsequently visualized under a laser confocal microscope (DMi8, Leica Microsystems, Wetzlar, Germany).

Mitoxox Immunohistochemistry

To assess the brain oxidative stress mitochondrial superoxide level, Mitoxox staining was performed using freshly frozen 8–10- μ m brain slices fixed on normal poly-L-lysine-coated slides. The slides were immersed in antigen retrieval solution (pH 6.0) and heated in a microwave for 15 min to unmask antigens. The slices were then dipped in 3% H₂O₂ for 10 min to block endogenous peroxidase. The slices were incubated with Mitoxox antibody (1:1000, Thermo Fisher, CA, USA) at room temperature. Six randomly selected regions per slice within the ipsilateral entorhinal cortex were examined under microscopic magnification of \times 200. The fluorescence intensity was quantified by ImageJ software (ImageJ 1.5, NIH, USA).

TUNEL Staining

Neuronal death was evaluated using TUNEL staining (In situ Apoptosis Detection Kit, 12,156,792,910, Roche, MO, USA) at 24 h after SAH according to the manufacturer's instructions. Under a fluorescence microscope (DMi8, Leica Microsystems, Wetzlar, Germany), TUNEL-positive neurons were counted under \times 200 magnification and averaged.

Nissl Staining

Brain slices (15 μ m thick) were submerged in 0.5% cresyl violet solution for 10 min until the desired intensity of staining was achieved. Hippocampal neuronal survival was evaluated based on neuronal morphology, as previously described [30]. The number of surviving neurons in three ipsilateral (left) hippocampal regions including cornu ammonis (CA1 and CA3), was counted under \times 200 magnification and averaged from 4 continuous brain slices/rat. The data were expressed as the number of surviving neurons per field.

Statistical Analysis

The data were expressed as mean \pm standard deviation (SD). Statistical analysis was performed using GraphPad Prism 8 (GraphPad Software, CA, USA). One-way or two-way ANOVA followed by Tukey's post hoc test was used for comparisons among multiple groups. Chi-square

Table 1 Summary of animal numbers and mortality

Groups	Mortality rate	Excluded
Experiment 1		
Sham	0% (0/8)	0
SAH (3 h, 6 h, 24 h, 72 h)	15.79% (6/38)	3
Experiment 2		
Sham	0% (0/10)	0
SAH + Vehicle	16.67% (2/12)	0
SAH + DY131 (2 mg/kg)	14.27% (1/7)	1
SAH + DY131 (6 mg/kg)	16.67% (2/12)	1
SAH + DY131 (18 mg/kg)	14.27% (1/7)	0
Experiment 3		
Sham	0% (0/10)	0
SAH + Vehicle	16.67% (2/12)	1
SAH + DY-131 (6 mg/kg)	16.67% (2/12)	0
Experiment 4		
Sham	0% (0/6)	0
SAH + Vehicle	0% (0/6)	0
SAH + DY131	0% (0/6)	1
SAH + DY131 + Vehicle	14.29% (1/7)	0
SAH + DY131 + GSK5182	14.29% (1/7)	0
SAH + DY131 + 3-TYP	0% (0/6)	0
Total		
Sham	0% (0/28)	0
SAH	13.64% (8/132)	7

test and *t*-test were used for comparisons between the two groups. A *P* value of less than 0.05 was considered statistically significant.

Results

Animal Experiment Results

No Difference in Animal Mortality and SAH Severity

As shown in Table 1, a total of 167 rats were used, of which 28 rats underwent a Sham operation and 139 underwent SAH induction. Out of 139 SAH rats, 7 rats were excluded because their SAH grading was less than 8 (mild SAH). The total mortality of SAH rats in the study was 13.64% (18/132). None of the rats died in the Sham-operated group. The SAH mortality rate was not significantly different among the experimental groups. The average SAH grades among all the SAH groups were not statistically different (Fig. 2B). Blood clots were mainly distributed around the Circle of Willis and the ventral brain stem after SAH induction, whereas no blood clot was observed in the brains of rats with Sham operation (Fig. 2A).

Temporal Increase in Endogenous ERR γ and SIRT3 Expressions in Brain and ERR γ Expression Colocalized with Neurons After SAH

A Western blot was performed to detect the protein levels of ERRs and SIRT3 in the left hemisphere among groups of Sham, 3, 6, 12, 24, and 72 h after SAH in rats. The results showed that the expression of ERR γ started increasing at 6 h and peaked at 24 h after SAH ($P < 0.05$; Fig. 2C, D). However, the expression of ERR α and ERR β did not

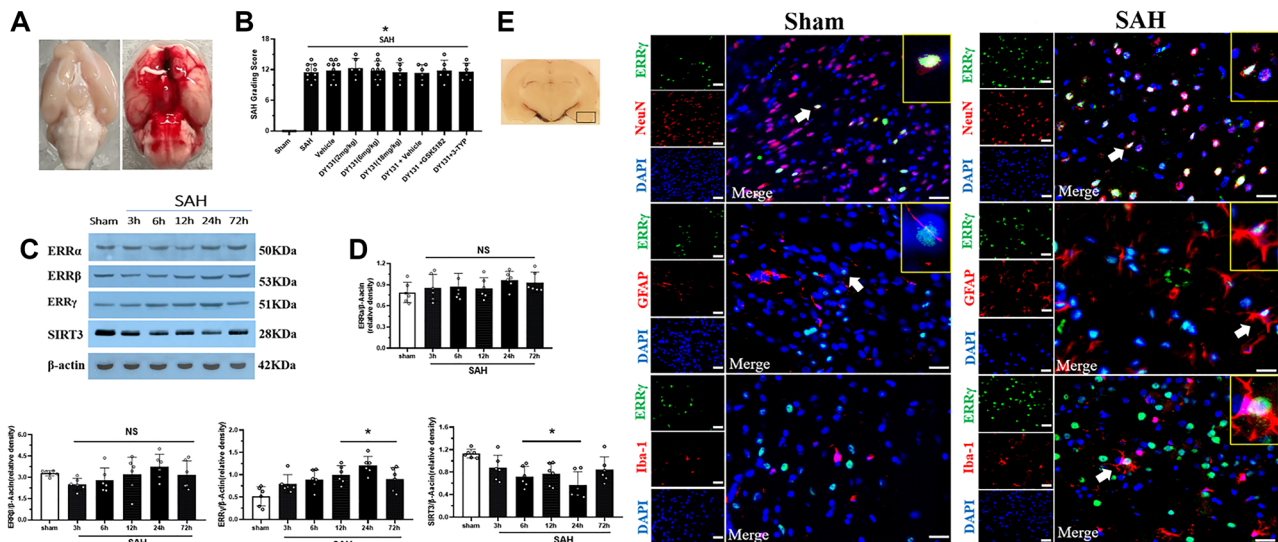


Fig. 2 The temporal expressions of ERRs and SIRT3 after SAH. **A** Representative pictures showed that subarachnoid blood clots were mainly presented around the circle of Willis in the rat brain at 24 h after SAH. **B** SAH grading scores of all SAH groups. **C**, **D** Representative Western blot bands of time course and densitometric quantification of ERR α , ERR β , ERR γ , and SIRT3. Data were represented

as mean \pm SD. $n = 6$ /group (A–D). **E** Immunofluorescence staining ERR γ (green) with neurons (NeuN, red), astrocytes (GFAP, red), and microglia (Iba-1, red) in the ipsilateral basal cortex at 24 h after SAH. Coronal brain slice indicates the location of the staining (small black box). Nuclei were stained with DAPI (blue). Scale bar = 50 μ m, $n = 2$ /group. One-way ANOVA, Tukey's post hoc test. * $P < 0.05$ vs. Sham group

change over time after SAH when compared with the Sham group ($P < 0.05$; Fig. 2C, D). The expression of SIRT3 dramatically decreased after SAH and reached the lowest level at 24 h when compared to the Sham group ($P < 0.05$; Fig. 2C, D). Double immunofluorescence staining of the ERR γ with the neuronal marker NeuN, astrocyte marker GFAP, or microglia marker Iba-1 showed that ERR γ receptors were primarily expressed in neurons and some in astrocytes and microglia in the rats, respectively. The number of ERR γ -positive cortical neurons was increased in the SAH (24 h) group compared with the Sham group (Fig. 2E). SIRT3 also showed an increase in the time course study of rats after SAH with a slight different peak time than that of ERR γ , suggesting the possible regulations by other upstream signaling in addition to ERR γ . Based on the findings of brain ERR subtype changes in SAH rats, this study focused on the role of ERR γ in SAH.

ERR γ Agonist DY131 Improved Short-term Neurobehavioral Deficits and Reduced Oxidative Stress Injury and Neuronal Apoptosis at 24 h After SAH

The neurobehavioral outcomes were evaluated 24 h after SAH. Rats in the SAH + Vehicle groups performed significantly

worse than Shams in the modified Garcia test and beam balance test ($P < 0.05$; Fig. 3D, E). The administration of DY131 (6 mg/kg or 18 mg/kg) significantly improved the neurological scores at 24 h after SAH. Given that DY131 was effective at a minimum dosage of 6 mg/kg, this dose was chosen for the following assessments of neuronal death/oxidative stress injury, long-term outcome, and molecular mechanisms.

TUNEL staining was used to evaluate the effect of DY131 on neuronal death 24 h after SAH. The TUNEL-positive neurons of the ipsilateral cortex in the SAH + Vehicle group were increased significantly compared with the Sham group 24 h after SAH, but the treatment of DY131 at a dose of 6 mg/kg significantly reduced the number of TUNEL-positive neurons ($P < 0.01$; Fig. 3A, B). Western blot data showed an increase in proapoptotic marker Bax and a decrease in anti-apoptotic marker Bcl-2 after SAH compared to Shams. DY131 treatment reduced the expression of Bax but enhanced the expression of Bcl-2 in SAH rats ($P < 0.01$; Fig. 3G, I, J). The oxidative stress level of the ipsilateral hemisphere after SAH was accessed by Mitosox staining and Western blot assessment of a marker of oxidative stress 4-HNE (Fig. 3A, C, G, H). The intensity of Mitosox staining and protein level of 4-HNE in the SAH + Vehicle group was greater compared with the Sham

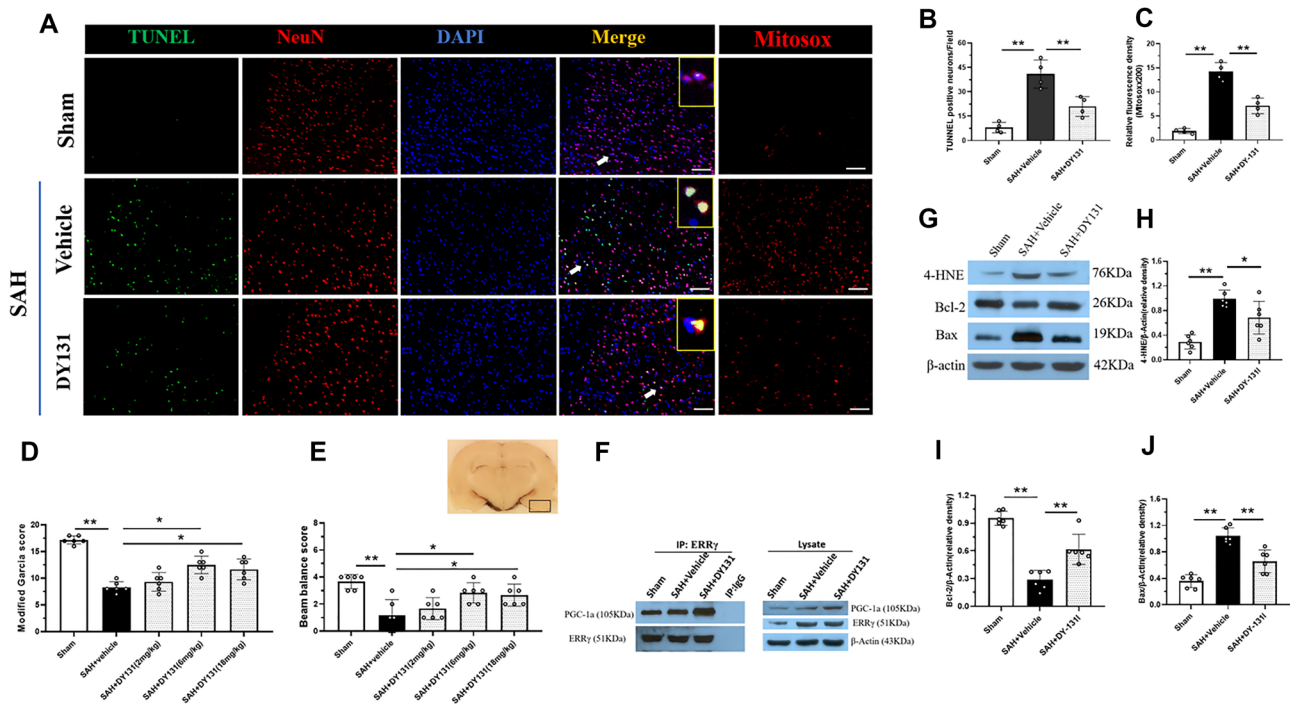


Fig. 3 DY131 (6 mg/kg, i.p. at 1 h post-SAH) improved short-term neurobehavioral deficits and reduced oxidative stress injury and neuronal apoptosis at 24 h after SAH. **A–C** Representative microphotographs of TUNEL and Mitosox immunofluorescence staining and quantitative analysis in the ipsilateral cortex of rat brain, $n=4$ per group. **D** Modified Garcia scores at 24 h after SAH. **E** Beam balance score at 24 h after SAH. **F** The effects of DY131 on the ERR γ /

PGC-1 α interaction after SAH. IP assay of ERR γ /PGC-1 α interaction in the left hemisphere at 24 h after SAH. **G–J** Representative Western blot bands and densitometric quantification of 4-HNE, Bcl-2, and Bax in the ipsilateral hemisphere at 24 h after SAH. $n=6$ per group (**D–J**). Vehicle: 10% dimethyl sulfide. Scale bar=100 μ m. Data were represented as mean \pm SD. One-way ANOVA Tukey’s post hoc test. * $P < 0.05$; ** $P < 0.01$

group 24 h after SAH. There were significantly lower Mitoxox staining intensity and 4-HNE protein levels in DY131-treated SAH rats, suggesting less oxidative stress injury.

ERR γ Agonist DY131 Increased the ERR γ /PGC-1 α Interaction at 24 h After SAH

Immunoprecipitation was applied to detect the ERR γ /PGC-1 α interaction regulated by DY131 treatment 24 h after SAH. The result showed that the ERR γ interacted with PGC-1 α in Shams and vehicle-treated SAH rats; however, DY131 treatment increased such interaction in SAH rats (Fig. 3F). These results suggested that DY131 facilitated the formation of ERR γ /PGC-1 α heterodimer.

DY131 Improved Long-term Neurological Functions and Reduced Hippocampal Neuronal Degeneration at 4 Weeks After SAH

The rotarod test showed that SAH remarkably impaired the rotarod test performance at both 5 and 10 RPM acceleration velocities compared with the Shams (Fig. 4A). DY131 treatment significantly increased the falling latency of both acceleration velocity at the first 2 weeks and that of 5 RPM acceleration velocity in the third week in SAH rats but not

the falling latency of 10 RPM acceleration velocity at the third week after SAH ($P < 0.01$; Fig. 4A). In the Morris water maze test, SAH impaired the spatial memory and learning ability with a longer escape latency and swimming distance to the platform than Shams on days 24 to 27 after SAH ($P < 0.01$; Fig. 4B). DY131 treatment significantly shortened escape latency on days 25 to 27 with reduced swimming distance on days 26 to 27 after SAH, compared with the SAH + Vehicle group ($P < 0.01$; Fig. 4B). In the probe trials, the rats in the SAH + Vehicle group stayed at significantly shorter duration within the probe quadrant, compared with the Sham ($P < 0.01$; Fig. 4C, D). However, DY131 treatment significantly increased the quadrant duration ($P < 0.01$; Fig. 4C, D). A significant difference was not observed in swimming speed between groups (Fig. 4E).

The hippocampus plays an important role in memory formation [31, 32], Nissl staining was performed in brain slices at the level of the hippocampus at 28 days after SAH. Within the CA1 and CA3 regions of the ipsilateral hippocampus, there was significantly more neuron loss and shrinkage morphology of neurons in the SAH + Vehicle group compared with the Sham group. DY131 treatment significantly reversed such neuronal damage in CA1 and CA3 regions of the ipsilateral hippocampus when compared to the SAH + Vehicle group ($P < 0.01$; Fig. 4F, G).

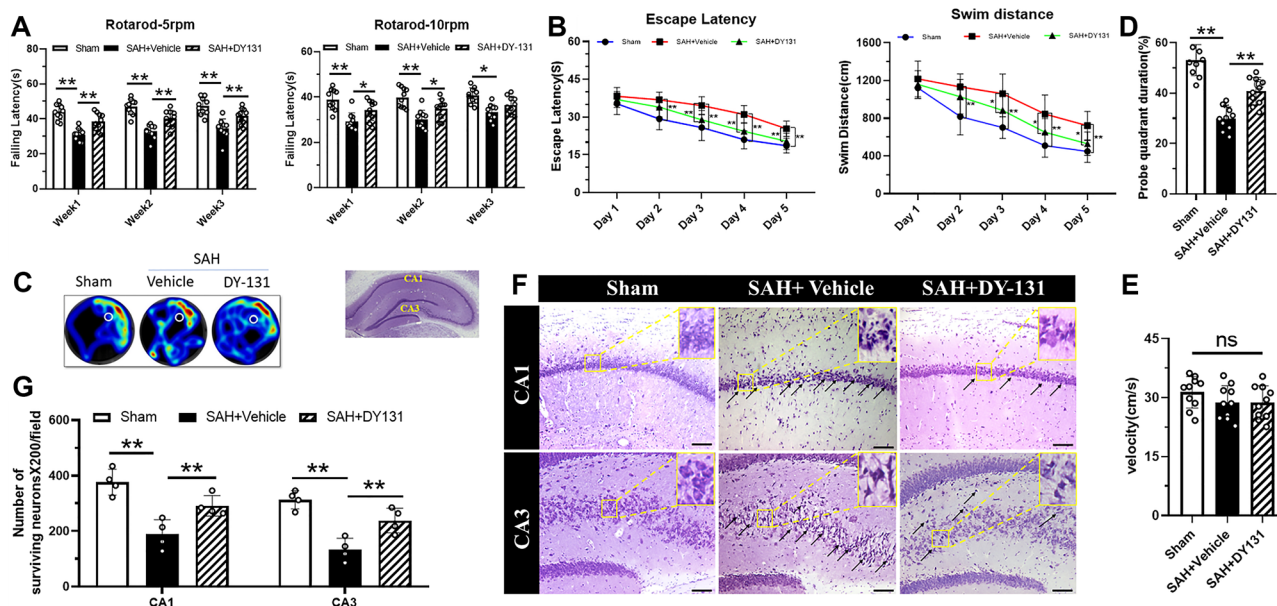


Fig. 4 DY131 (6 mg/kg, i.p. at 1 h, 24 h, 48 h, and 72 h post-SAH) treatment improved the long-term outcomes at 28 days after SAH. **A** Rotarod test of 5 rpm and 10 rpm. **B** Escape latency and swim distance of water maze test. **C** Representative heat map in the probe test showed DY131-treated SAH spent more time in the probe quadrant. **D** Probe quadrant duration. **E** Velocity of probe trial. $n = 10$ /group (**A**–

E). **F**, **G** Representative images and neuronal quantifications of Nissl staining in hippocampal CA1 and CA3 regions. Arrows indicate shrunken pyramidal or dead neurons. Scale bar = 100 μ m, $n = 4$ /group. Data were expressed as mean \pm SD. Two-way ANOVA, Tukey's post hoc test for (**A**, **B**, **G**). One-way ANOVA, Tukey's post hoc test for (**D**, **E**). * $P < 0.05$; ** $P < 0.01$

Selective EER γ Inhibitor GSK5182 and SIRT3 Inhibitor 3-TYP Abolished the Neuroprotective Effects of DY131 and Its Regulation on PGC-1 α /SIRT3 Protein Levels at 24 h After SAH

To verify the EER γ activation involved in the neuroprotective effects of DY131 post-SAH, the specific EER γ antagonist GSK5182 was injected via icv to inhibit the EER γ . To verify the role of SIRT3 in EER γ -mediated neuroprotection, 3-TYP (a specific inhibitor of SIRT3) was administered via icv prior to DY131 administration. Without affecting the EER γ protein level, DY131 further increased protein levels of PGC-1 α , SIRT3, and Bcl-2 but decreased Ac-SOD, 4-HNE, and Bax in SAH rats when compared with those in the SAH + Vehicle group ($P < 0.05$; Fig. 5A–H). EER γ inhibitor GSK5182 reversed these effects of DY131 after SAH ($P < 0.05$; Fig. 5A–H). As shown in Fig. 5A–H, GSK5182 decreased the downstream protein levels, including SIRT3 and Bcl-2 in the SAH + DY131 + GSK5182 group compared with those in the SAH + DY131 + DMSO group. Consistently, significant overexpression of Ac-SOD, 4-HNE, and Bax was observed in the SAH + DY131 + GSK5182 group when compared with the SAH + DY131 + DMSO group ($P < 0.05$; Fig. 5A–H). However, inhibiting SIRT3 by 3-TYP abolished the effects of DY131 on Ac-SOD, 4-HNE, Bax, and Bcl-2 ($P < 0.05$; Fig. 5A–H) but not the expressions of PGC-1 α and SIRT3 (Fig. 5A–H).

Cell Experiment Results

Cell Density

Immunofluorescence staining was used to identify the purity of neuronal cells in the primary neuronal culture. As shown in Fig. 6A, more than 90% of DAPI-stained cultured cells (blue) were NeuN cells (red), suggesting the success of the primary neuronal culture. Exposing neuronal cells to 0.3 mg/ml of Hb caused cell detachment in a time-dependent manner. The cell viability assay showed that $64.0 \pm 8.9\%$ of cells were attached to the plates after 24 h of incubation with Hb, but only $43.6 \pm 6.7\%$ of cells were still attached after 72 h. EER γ agonist DY131 failed to protect cells at a lower concentration (2.5–5 μ M) but significantly prevented cell detachment at a higher concentration (10–20 μ M) ($P < 0.05$; Fig. 6B, C). Therefore, 10 μ M (EER γ agonist DY131) was selected as the optimal dose for cell experiments in subsequent experiments.

EER γ Knockdown Reversed Protective Effects of DY131 Against Hb-induced Neuronal Toxicity In Vitro

The knockdown of endogenous EER γ with siRNA was verified using Western blot and immunofluorescence. The protein level of neuronal EER γ was significantly decreased by EER γ siRNA compared to scramble siRNA ($P < 0.05$;

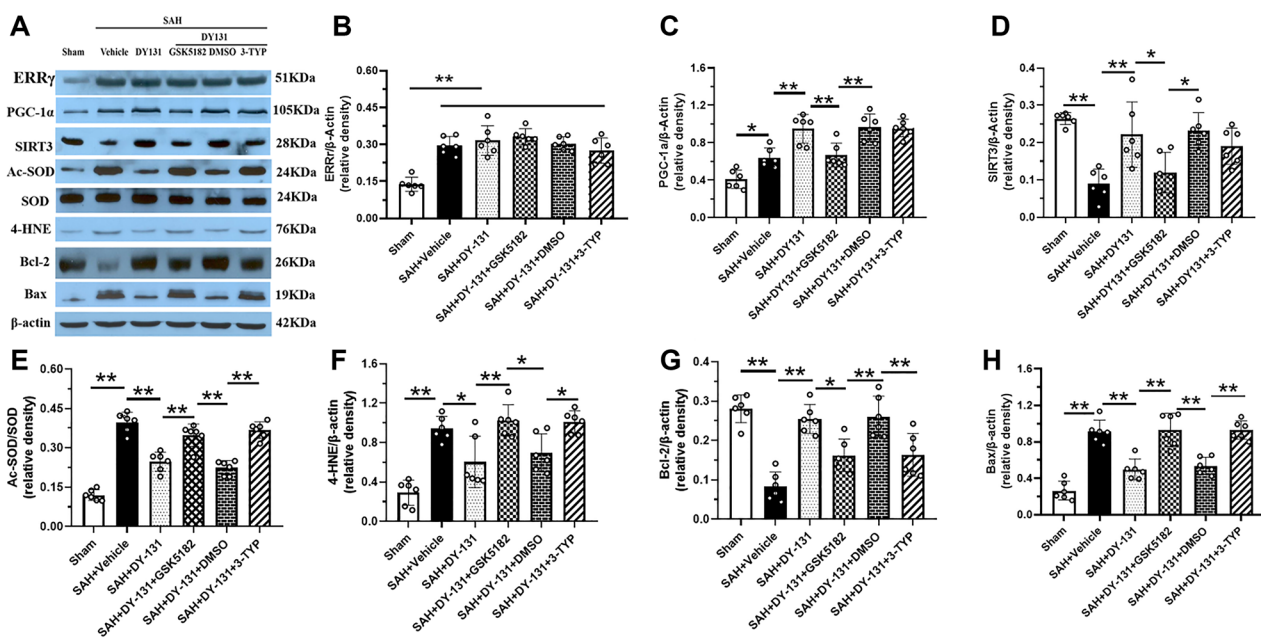


Fig. 5 Selective EER γ inhibitor GSK5182 (12 μ mol/ml, i.c.v. at 1 h prior to SAH induction) and SIRT3 inhibitor 3-TYP (40 μ mol/ml, i.c.v. at 1 h prior to SAH induction) abolished the neuroprotective effects of DY131 (6 mg/kg, i.p. at 1 h post-SAH) and its regulation on PGC-1 α /SIRT3 protein levels at 24 h after SAH. **A–H** Representa-

tive Western blot bands and densitometric quantification of EER γ , PGC-1 α , SIRT3, Ac-SOD, SOD, 4-HNE, Bcl-2, and Bax in the ipsilateral hemisphere at 24 h after SAH. $n = 6$ /group. Data were shown as means \pm SD. One-way ANOVA, Tukey's post hoc test. * $P < 0.05$; ** $P < 0.01$

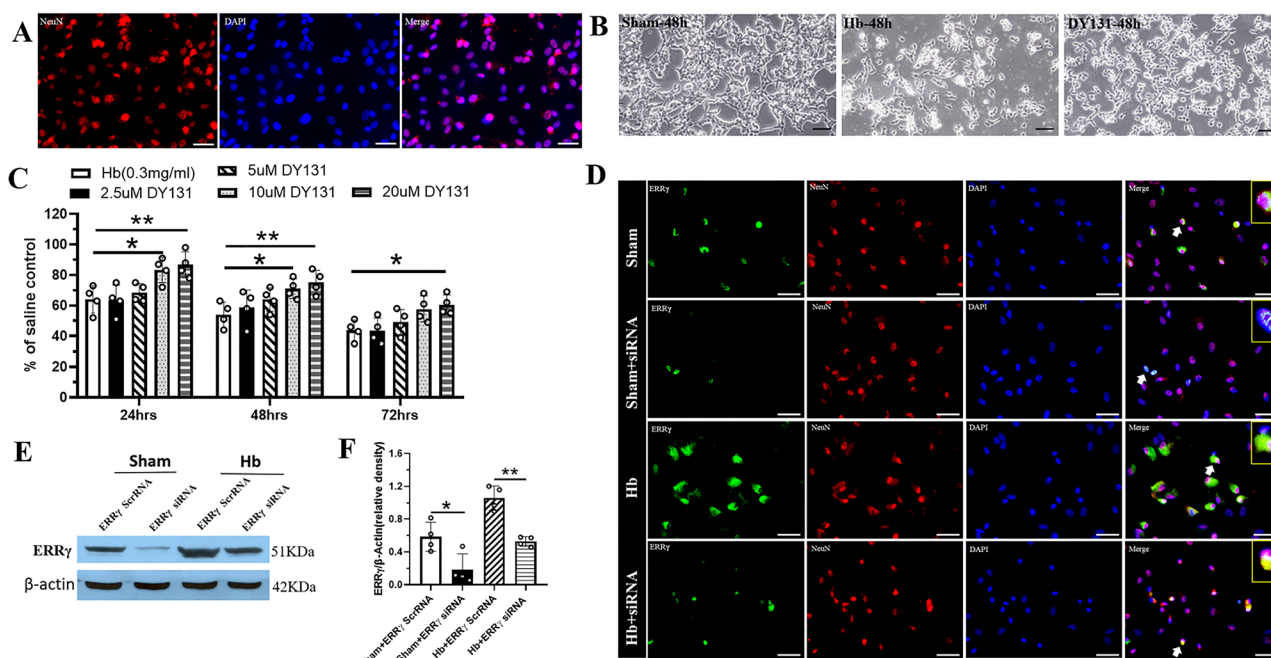


Fig. 6 DY131 (10 μ M, preincubated for 30 min prior to Hb exposure and cocubated with Hb for 24 h, 48 h, or 72 h) attenuated Hb-induced neuronal toxicity in vitro and effects of ERR γ siRNA knockout. **A** Primary neuron culture shown by immunofluorescence staining with NeuN and DAPI. Scale bar=50 μ m. **B** Cell morphology. Scale bar=100 μ m. **C** Quantitative analysis of cell viability among different time points after SAH; * P <0.05 compared with Hb

(alone)-treated cells. **D** Immunofluorescence staining ERR γ (green) with neurons (NeuN, red) in neurons at 48 h in the Sham group or Hb group. Nuclei were stained with DAPI (blue). Scale bar=50 μ m, n =4/group. **E**, **F** Representative Western blot bands and densitometric quantification of ERR γ demonstrated the efficacy of siRNA knockout in Sham and Hb group, n =4/group. One-way ANOVA, Tukey's post hoc test. * P <0.05; ** P <0.01

Fig. 6D–F). To further verify if the ERR γ mediated the neuroprotective effects of DY131, Western blots were performed at 48 h after Hb exposure. The protein level of neuronal ERR γ was significantly decreased by ERR γ siRNA compared to scramble siRNA (P <0.05; Fig. 7B). The protein levels of Bcl-2 were lower but those of Bax were greater in the Hb exposure + DY131 + ERR γ siRNA group when compared with Hb exposure + DY131 + ScrRNA group (P <0.05; Fig. 7B, G, H). The results suggested that ERR γ knockdown by ERR γ siRNA reversed the anti-apoptotic effects of DY131 in the cell culture model of Hb-induced neuronal toxicity.

Consistently, Hb exposure significantly increased the TUNEL-positive cells in the Hb + Vehicle group (P <0.01, Fig. 7A, C). ERR γ knockdown by ERR γ siRNA reversed the DY131 protection against neuronal death in the Hb + DY131 + ERR γ siRNA group when compared with the Hb + DY131 + ScrRNA group (P <0.05, Fig. 7A). The oxidative stress level was accessed by Mitosox staining as well as the Western blot measurements of 4-HNE (a marker of oxidative stress). The intensity of Mitosox staining and the protein level of 4-HNE in the Hb + Vehicle group were greater compared with the Sham group (P <0.01, Fig. 7A, D, F). There were significantly lower Mitosox staining intensity

and 4-HNE protein levels in Hb + DY131 group, suggesting less oxidative injury (P <0.01, Fig. 7A, D, F). Similarly, Mitosox staining and Western blot results revealed that ERR γ siRNA increased Mitosox staining intensity and 4-HNE protein levels in the Hb + DY131 + ERR γ siRNA group when compared with the Hb + DY131 + ScrRNA group (P <0.01, Fig. 7A, D, F).

Human study-Increased Expressions of ERR γ and Neuronal Apoptosis Marker CC3 in the Brain Tissues of SAH Patients, Demonstrating the Clinical Relevance of ERR γ Target

We examined the expression of ERR γ and cleaved caspase-3 (CC3) in the brain tissues resected from SAH patients. Compared with the non-SAH control samples, the levels of ERR γ and CC3 were significantly higher in the brain tissues resected from SAH patients (P <0.01; Fig. 8C, G, H). Similarly, Immunohistochemistry (IHC) staining showed that the expressions of ERR γ and CC3 on brain sections of SAH patients were higher than that in the non-SAH brain tissues (P <0.01; Fig. 8D–F). Consistent with the previous reports, it suggests that ERR γ might be involved in the neuronal apoptotic process in SAH patients.

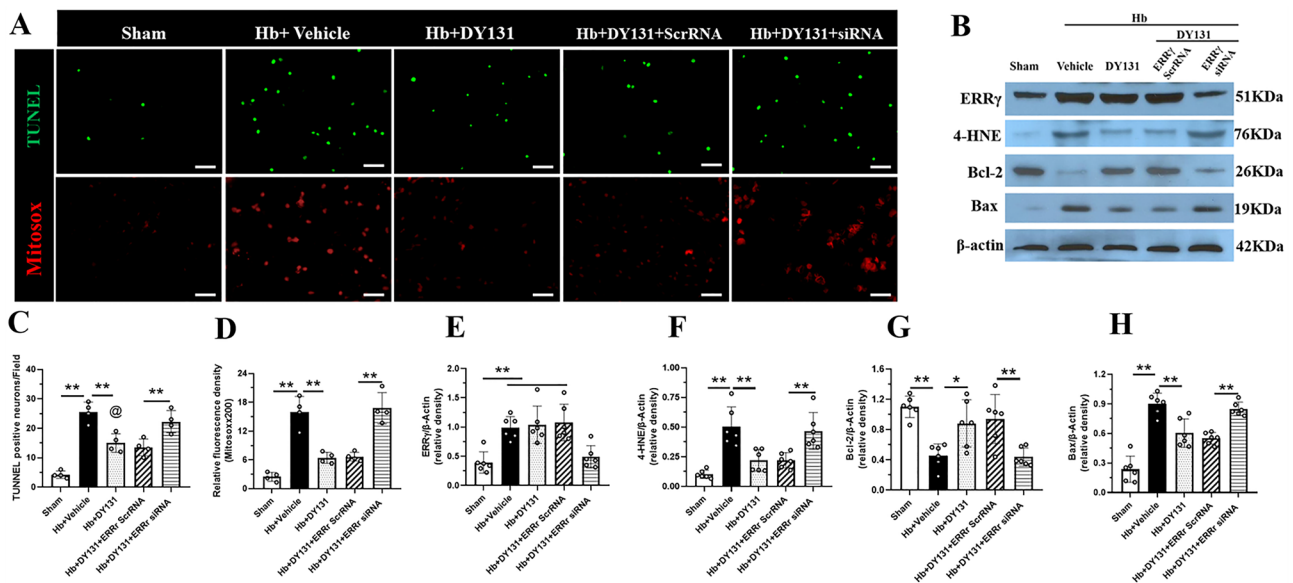


Fig. 7 ERR γ siRNA knockout abolished the beneficial effect of DY131 in vitro. **A, C, D** Representative microphotographs of TUNEL and Mitosox immunofluorescence staining and quantitative analysis for Mitosox and TUNEL-positive cells in vitro. Scale bar = 100 μ m. *n* = 4/group. **B, E–H** Representative Western blot bands

and densitometric quantification of ERR γ , 4-HNE, Bcl-2, and Bax at 48 h after Hb. Vehicle: 10% dimethyl sulfide, *n* = 6/group. Data were represented as mean \pm SD. One-way ANOVA. Tukey's post hoc test. **P* < 0.05; ***P* < 0.01

Discussion

Despite a great number of pharmacological neuroprotectants that have been researched and developed, no significant progress has been made in clinical or basic research, unfortunately, due to the complicated pathological mechanisms of SAH [4]. Thus, exploring effective neuroprotectants is an extreme clinical demand. In our study, we for the first time explored the neuroprotective effects of DY131 against oxidative stress and neuronal apoptosis in EBI and the potential mechanisms involving the ERR γ /PGC-1 α /SIRT3 signaling pathway after SAH (Fig. 9).

Mitochondria directly control cell survival and death by maintaining energy homeostasis and regulating redox-dependent signaling pathways [33]. Mitochondrial dysfunction leads to an increase in ROS, which induces damage to lipids, proteins, and DNA [34]. Mitochondria themselves are also vulnerable to oxidative injury [35]. After SAH, a large amount of hemoglobin is released into the cerebrospinal fluid (CSF), where it can react with neuronal cells. Extracellular hemoglobin is a powerful oxidant [36], and extracellular iron released from hemoglobin can generate free radicals via the Fenton reaction (37). In the current study, we used a rat model of endovascular perforation [23] in vivo and Hb exposure-induced neuronal toxicity in primary cortical neuron culture [38] to mimic such pathology of SAH.

The ERR γ activation promotes energy-generating mitochondrial functions in several energy-demanding cell types,

including neurons, cardiomyocytes, skeletal myocytes, and renal epithelial cells [11, 18, 39, 40]. Responding to hypoxia, there is an upregulation of ERR γ -mediated metabolic responses [41, 42]. Hippocampal function is dependent on ERR γ -regulated mitochondrial metabolism [18, 43]. In our study, the increases in neuronal expressions of ERR γ in SAH rats suggest its participation in the endogenous neuroprotection mechanisms after SAH. However, such endogenous activation appears not to be sufficient to overcome SAH injury. Exogenous pharmacological activation is desired.

DY131 is a selective agonist that can induce the transcriptional activity of ERR γ and regulate ERR γ -mediated metabolism [19, 20]. It is able to readily penetrate the blood–brain barrier due to the hydrophobic feature and a topological surface area (TPSA) of less than 70 [20]. Recent studies demonstrated that DY131 could attenuate oxidative stress, inflammation, and apoptosis, leading to overall protection against LPS-induced acute liver injury [21]. Similarly, we found that DY131 treatment significantly reduced short- and long-term neurologic deficits and improved memory/spatial learning after SAH. The use of 10.0 μ M DY131 significantly reduced Hb-induced neuronal toxicity and increased cell viability.

The hippocampal damage could cause cognitive and memory impairments after SAH [31, 32]. The neurodegeneration of hippocampal CA1 and CA3 was evident at 28 days after SAH in rats. The previous study showed that mice with neuronal ERR γ deficiency in the cerebral cortex and hippocampus exhibited impaired spatial learning and

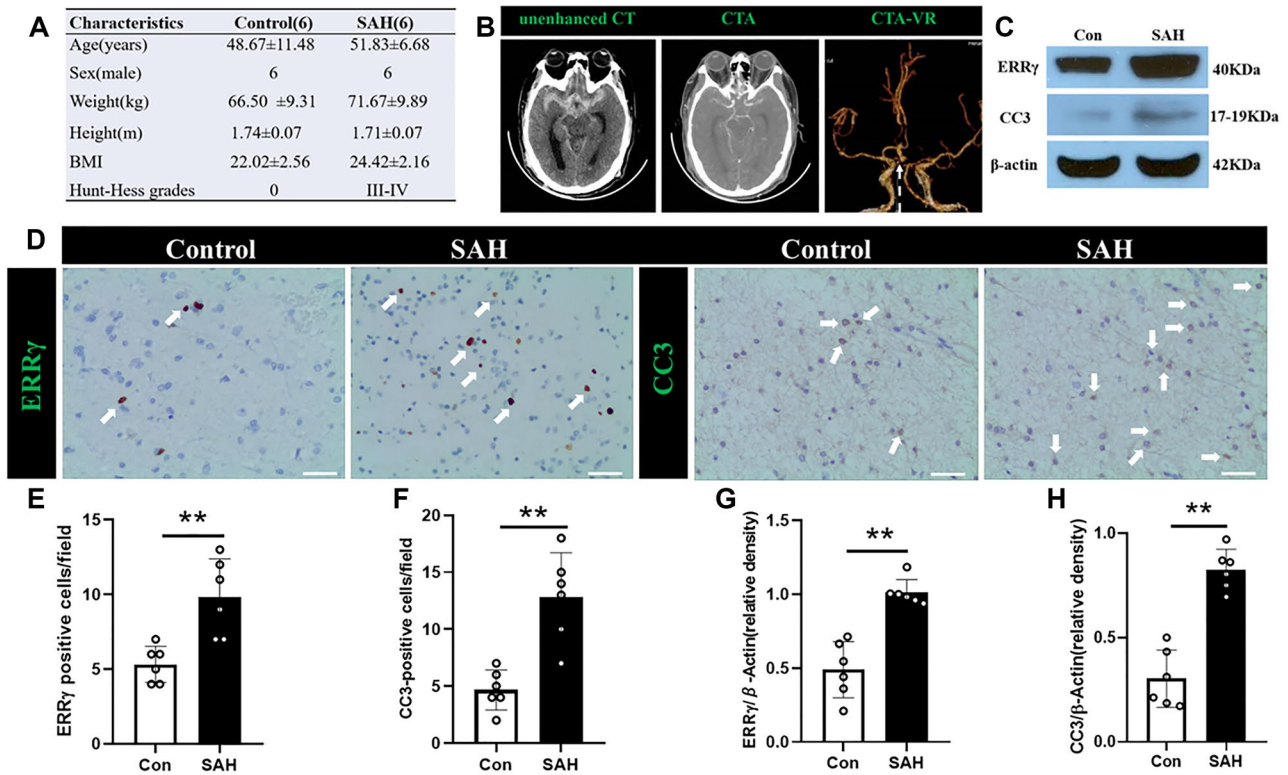


Fig. 8 Expressions of ERR γ and CC3 in the brain tissues of SAH patients. **A** Clinical characteristics of SAH patients and controls. **B** Representative CT scanning images showing blood distribution and aneurysm in a SAH patient. An unenhanced axial CT image (left) shows hemorrhagic densities in the brain cistern; a CTA axial image (middle) and CTA-VR image (right) show the posterior communicat-

ing aneurysm in the patient (arrow). **D–F** IHC staining and densitometric quantification of ERR γ and CC3 on patient brain sections after SAH. Scale bar = 200 μ m. **C**, **G**, **H** Representative Western blot bands and densitometric quantification of ERR γ and CC3 in patient brain tissue after SAH. $n = 6$ /group. Data were represented as mean \pm SD. Chi-square test and t -test. * $P < 0.05$; ** $P < 0.01$

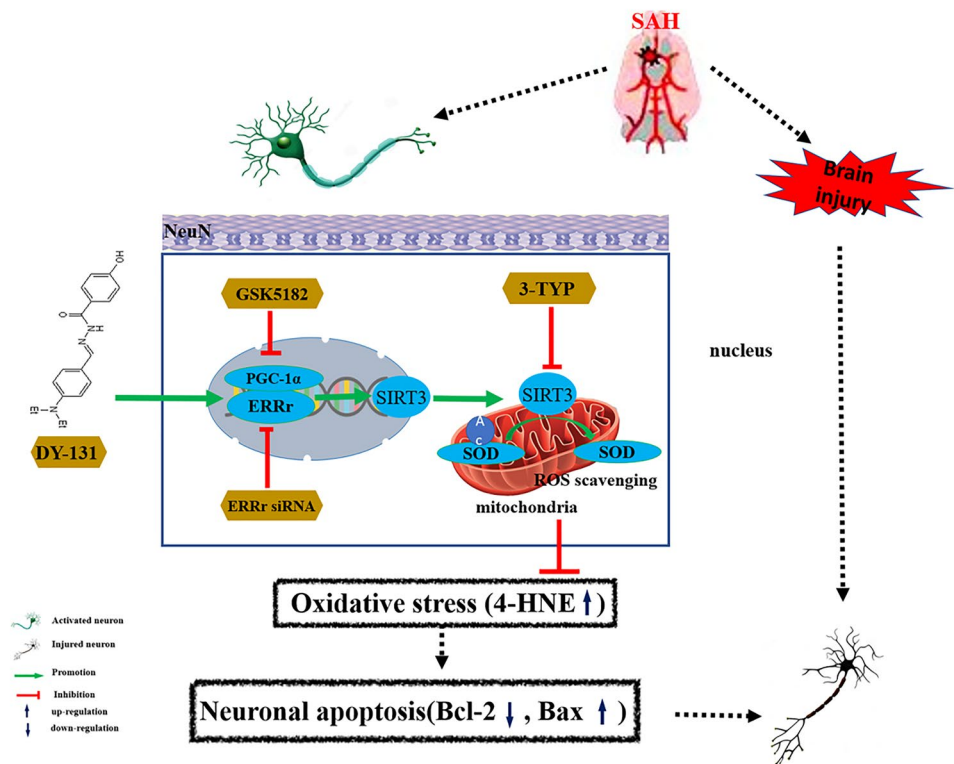
memory [18]. In the present study, DY131 treatment significantly mitigated the neuronal degeneration in CA1 and CA3, as measured by Nissl staining, and improved long-term neurobehavioral functions. The long-term protection may be attributed to the attenuated EBI by ERR γ activation in SAH rats.

PGC-1 α is a master regulator to regulate mitochondrial biogenesis; it mainly upregulates mitochondrial DNA and induces the expression of genes encoding mitochondrial proteins [44, 45]. The PGC-1 α functions in the regulation of oxidative metabolism are mediated through the ERRs [46, 47]. Recent studies indicated that the PGC-1 α activation resulted in a protective effect by increasing the expressions of mitochondrial antioxidants SOD2 in animal models of Parkinson's disease (PD) [48]. As a downstream target gene of PGC-1 α , SIRT3 is typically localized in mitochondria and integrates its role in regulating mitochondrial function related to metabolic enzyme activity, oxidative phosphorylation, and anti-oxidant machinery [49]. Both in vitro and in vivo studies demonstrated that SIRT3 produced beneficial effects in cerebrovascular disease models [50, 51]. A selective SIRT3 inhibitor, 3-TYP, inhibited melatonin-enhanced

SIRT3 activity but did not affect SIRT3 protein expression. It significantly attenuates melatonin-induced increases in deacetylated-SOD2 expression and SOD2 activity in HepG2 cells exposed to Cd [52, 53]. Our results indicated that DY131 treatment significantly increased the ERR γ /PGC-1 α interaction and upregulated the expression of SIRT3, leading to the downregulation of the oxidative stress marker 4-HNE and Ac-SOD as well as proapoptotic marker Bax at 24 h after the experimental SAH. The application of GSK5182, a selective ERR γ antagonist [54], or a selective SIRT3 inhibitor 3-TYP reverse the effects of DY131 treatment on PGC-1 α /SIRT3 signaling at 24 h after SAH in rats, suggesting SIRT3 acts as downstream signaling of ERR γ activation.

There are some limitations in this study. First, previous studies and our own data show ERR α may be involved in the pathophysiological process in SAH patients. The role of ERR α in the pathophysiological changes of SAH needs to be further studied [18]. Second, previous studies have demonstrated that ERR γ activation could regulate neuronal differentiation via GSK3 β /NFAT signaling [55]. Thus, the contribution of other signaling pathways to the anti-oxidative stress and anti-apoptotic effects of ERR γ

Fig. 9 The graphic abstract. The DY131 attenuates oxidative stress and neuronal apoptosis via ERR γ /PGC-1 α /SIRT3 pathway after SAH



activation cannot be excluded. Third, DY131 administration was only applied at a single time point (1 h after SAH). The optimal therapeutic window of DY131 treatment for SAH was not evaluated in the present study. Fourth, sex differences are not investigated. Lastly, corrections for multiple comparisons were not used.

Collectively, our findings provided a new insight into the neuroprotective effects of ERR γ activation against EBI after SAH. ERR γ agonist DY131 ameliorated oxidative stress and neuronal apoptosis both in vitro and in vivo, leading to the improvement of neurobehavioral impairments after SAH in rats. The effects were at least partially mediated by the ERR γ /PGC-1 α /SIRT3 signaling pathway. These findings suggest that ERR γ may serve as a potential therapeutic target for SAH patients.

Supplementary Information The online version contains supplementary material available at <https://doi.org/10.1007/s13311-022-01330-8>.

Acknowledgements This work was supported by grants from the National Institutes of Health (NS081740 and NS082184) to John H. Zhang.

Required Author Forms Disclosure forms provided by the authors are available with the online version of this article.

Declarations

Conflict of Interest The authors declare no conflict of interest.

References

- van Gijn J, Kerr RS, Rinkel GJE. Subarachnoid haemorrhage. *Lancet*. 2007;369:306–18.
- Neifert SN, Chapman EK, Martini ML, Shuman WH, Schupper AJ, Oermann EK, et al. Aneurysmal subarachnoid hemorrhage: the last decade. *Transl Stroke Res*. 2021;12:428–46.
- Cahill WJ, Calvert JH, Zhang JH. Mechanisms of early brain injury after subarachnoid hemorrhage. *J Cereb Blood Flow Metab*. 2006;26:1341–53.
- Fumoto T, Naraoka M, Katagai T, Li Y, Shimamura N, Ohkuma H. The role of oxidative stress in microvascular disturbances after experimental subarachnoid hemorrhage. *Transl Stroke Res*. 2019;10:684–94.
- Mao L, Wang K, Zhang P, Ren S, Sun J, Yang M, et al. Carbonyl reductase 1 attenuates ischemic brain injury by reducing oxidative stress and neuroinflammation. *Transl Stroke Res*. 2021; 12:711–24.
- Tsai TH, Lin SH, Wu CH, Tsai YC, Yang SF, Lin CL. Mechanisms and therapeutic implications of RTA 408, an activator of Nrf2, in subarachnoid hemorrhage-induced delayed cerebral vasospasm and secondary brain injury. *PLoS ONE*. 2020. <https://doi.org/10.1371/journal.pone.0240122>.
- Hwang JA, Shin N, Shin HJ, Yin Y, Kwon HH, Park H, et al. Protective effects of ShcA protein silencing for photothrombotic cerebral infarction. *Transl Stroke Res*. 2021;12:866–78.
- Deblois G, Smith HW, Tam IS, Gravel SP, Caron M, Savage P, et al. ERR α mediates metabolic adaptations driving lapatinib resistance in breast cancer. *Nat Commun*. 2016. <https://doi.org/10.1038/ncomms12156>.
- Vernier M, Dufour CR, McGuirk S, Scholtes C, Li X, Bourmeau G, et al. Estrogen-related receptors are targetable ROS sensors. *Genes Dev*. 2020;34:544–59.

10. Charest-Marcotte A, Dufour CR, Wilson BJ, Tremblay AM, Eichner LJ, Arlow DH, et al. The homeobox protein Prox1 is a negative modulator of ERR α /PGC-1 α bioenergetic functions. *Genes Dev.* 2010;24:537–42.
11. Dufour CR, Wilson BJ, Huss JM, Kelly DP, Alaynick WA, Downes M, et al. Genome-wide orchestration of cardiac functions by the orphan nuclear receptors ERR α and γ . *Cell Metab.* 2007;5:345–56.
12. Scholtes C, Giguère V. Transcriptional regulation of ROS homeostasis by the ERR subfamily of nuclear receptors. *Antioxidants.* 2021;10:1–19.
13. Birben E, Sahiner UM, Sackesen C, Erzurum S, Kalayci O. Oxidative stress and antioxidant defense. *World Allergy Organ J.* 2012;5:9–19.
14. Valle I, Álvarez-Barrientos A, Arza E, Lamas S, Monsalve M. PGC-1 α regulates the mitochondrial antioxidant defense system in vascular endothelial cells. *Cardiovasc Res.* 2005;66:562–73.
15. Vazquez A, Tedeschi PM, Bertino JR. Overexpression of the mitochondrial folate and glycine-serine pathway: A new determinant of methotrexate selectivity in tumors. *Can Res.* 2013;73:478–82.
16. Lebleu VS, O'Connell JT, Gonzalez Herrera KN, Wikman H, Pantel K, Haigis MC, et al. PGC-1 α mediates mitochondrial biogenesis and oxidative phosphorylation in cancer cells to promote metastasis. *Nat Cell Biol.* 2014;16:992–1003.
17. Gofflot F, Chartoire N, Vasseur L, Heikkinen S, Dembele D, le Merrer J, et al. Systematic gene expression mapping clusters nuclear receptors according to their function in the brain. *Cell.* 2007;131:405–18.
18. Pei L, Mu Y, Leblanc M, Alaynick W, Barish GD, Pankratz M, et al. Dependence of hippocampal function on ERR γ -regulated mitochondrial metabolism. *Cell Metab.* 2015;21:628–36.
19. Huang B, Mu P, Yu Y, Zhu W, Jiang T, Deng R, et al. Inhibition of EZH2 and activation of ERR γ synergistically suppresses gastric cancer by inhibiting FOXM1 signaling pathway. *Gastric Cancer.* 2021;24:72–84.
20. Yu DD, Forman BM. Identification of an agonist ligand for estrogen-related receptors ERR β / γ . *Bioorg Med Chem Lett.* 2005;15:1311–3.
21. Ma H, Liu J, Du Y, Zhang S, Cao W, Jia Z, et al. Estrogen-related receptor γ agonist DY131 ameliorates lipopolysaccharide-induced acute liver injury. *Front Pharmacol.* 2021. <https://doi.org/10.3389/fphar.2021.626166>.
22. Li H, Wu W, Sun Q, Liu M, Li W, Zhang XS, et al. Expression and cell distribution of receptor for advanced glycation end-products in the rat cortex following experimental subarachnoid hemorrhage. *Brain Res.* 2014;1543:315–23.
23. Sugawara T, Ayer R, Jadhav V, Zhang JH. A new grading system evaluating bleeding scale in filament perforation subarachnoid hemorrhage rat model. *J Neurosci Methods.* 2008;167:327–34.
24. Kim HJ, Kim BK, Ohk B, Yoon HJ, Kang WY, Cho S, et al. Estrogen-related receptor γ negatively regulates osteoclastogenesis and protects against inflammatory bone loss. *J Cell Physiol.* 2019;234:1659–70.
25. Zhou K, Enkhjargal B, Xie Z, Sun C, Wu L, Malaguit J, et al. Dihydropyridic acid inhibits lysosomal rupture and NLRP3 through lysosome-associated membrane protein-1/calcium/calmodulin-dependent protein kinase II/TAK1 pathways after subarachnoid hemorrhage in rat. *Stroke.* 2018;49:175–83.
26. Redmond L, Kashani AH, Ghosh A. Calcium regulation of dendritic growth via CaM kinase IV and CREB-mediated transcription. *Neuron.* 2002;34:999–1010.
27. Meguro T, Chen Betty, Parent AD, Zhang JH. Caspase inhibitors attenuate oxyhemoglobin-induced apoptosis in endothelial cells. *Stroke.* 2001;32:61–6.
28. Bromley-Brits K, Deng Y, Song W. Morris Water maze test for learning and memory deficits in Alzheimer's disease model mice. *J Vis Exp.* 2011. <https://doi.org/10.3791/2920>.
29. Mahmood T, Yang PC. Western blot: Technique, theory, and trouble shooting. *N Am J Med Sci.* 2012;4:429–34.
30. Okada T, Enkhjargal B, Travis ZD, Ocak U, Tang J, Suzuki H, et al. FGF-2 attenuates neuronal apoptosis via FGFR3/PI3k/Akt signaling pathway after subarachnoid hemorrhage. *Mol Neurobiol.* 2019;56:8203–19.
31. Veldeman M, Coburn M, Rossaint R, Clusmann H, Nolte K, Kremer B, et al. Xenon reduces neuronal hippocampal damage and alters the pattern of microglial activation after experimental subarachnoid hemorrhage: A randomized controlled animal trial. *Front Neurol.* 2017. <https://doi.org/10.3389/fneur.2017.00511>.
32. Wong FCC, Yatawara C, Low A, Foo H, Wong BYX, Lim L, et al. Cerebral small vessel disease influences hippocampal subfield atrophy in mild cognitive impairment. *Transl Stroke Res.* 2021;12:284–92.
33. Galluzzi L, Kepp O, Kroemer G. Mitochondria: Master regulators of danger signalling. *Nat Rev Mol Cell Biol.* 2012;13:780–8.
34. Adiele RC, Adiele CA. Metabolic defects in multiple sclerosis. *Mitochondrion.* 2019;44:7–14.
35. Lin MT, Beal MF. Mitochondrial dysfunction and oxidative stress in neurodegenerative diseases. *Nature.* 2006;443:787–95.
36. Bamm VV, Lanthier DK, Stephenson EL, Smith GST, Harauz G. In vitro study of the direct effect of extracellular hemoglobin on myelin components. *Biochim Biophys Acta Mol Basis Dis.* 2015;1852:92–103.
37. Panfoli I, Candiano G, Malova M, de Angelis L, Cardiello V, Buonocore G, et al. Oxidative stress as a primary risk factor for brain damage in preterm newborns. *Front Pediatr.* 2018. <https://doi.org/10.3389/fped.2018.00369>.
38. Meguro T, Chen B, Lancon J, Zhang JH. Oxyhemoglobin induces caspase-mediated cell death in cerebral endothelial cells. *J Neurochem.* 2001;77:1128–35.
39. Narkar VA, Fan W, Downes M, Yu RT, Jonker JW, Alaynick WA, et al. Exercise and PGC-1 α -independent synchronization of type I muscle metabolism and vasculature by ERR γ . *Cell Metab.* 2011;13:283–93.
40. Zhao J, Lupino K, Wilkins BJ, Qiu C, Liu J, Omura Y, et al. Genomic integration of ERR γ -HNF1 β regulates renal bioenergetics and prevents chronic kidney disease. *Proc Natl Acad Sci USA.* 2018;115:E4910–9.
41. Lee JH, Kim EJ, Kim DK, Lee JM, Park SB, Lee IK, et al. Hypoxia induces PDK4 gene expression through induction of the orphan nuclear receptor ERR γ . *PLoS ONE.* 2012. <https://doi.org/10.1371/journal.pone.0046324>.
42. Rangwala SM, Wang X, Calvo JA, Lindsley L, Zhang Y, Deyneko G, et al. Estrogen-related receptor γ is a key regulator of muscle mitochondrial activity and oxidative capacity. *J Biol Chem.* 2010;285:22619–29.
43. Hermans-Borgmeyer I, Èsens US, Borgmeyer U. Developmental expression of the estrogen receptor-related receptor g in the nervous system during mouse embryogenesis. *Mech Dev.* 2000;97:197–9.
44. Ventura-Clapier R, Garnier A, Veksler V. Transcriptional control of mitochondrial biogenesis: The central role of PGC-1 α . *Cardiovasc Res.* 2008;79:208–17.
45. Lv J, Deng C, Jiang S, Ji T, Yang Z, Wang Z, et al. Blossoming 20: The energetic regulator's birthday unveils its versatility in cardiac diseases. *Theranostics.* 2019;9:466–76.
46. Wu Z, Puigserver P, Andersson U, Zhang C, Adelmant G, Mootha V, Troy A, Cinti S, Lowell B, Scarpulla RC, Spiegelman BM. Mechanisms controlling mitochondrial biogenesis and respiration through the thermogenic coactivator PGC-1. *Cell.* 1999;98(1):115–24.
47. Schreiber SN, Emter R, Hock MB, Knutti D, Cardenas J, Podvinec M, et al. The estrogen-related receptor (ERR) functions in PPAR coactivator 1 (PGC-1)-induced mitochondrial biogenesis. *Proc Natl Acad Sci U S A.* 2004;101:6472–7. <https://doi.org/10.1073/pnas.0308686101>.

48. Mudò G, Mäkelä J, di Liberto V, Tselykh TV, Olivieri M, Piepponen P, et al. Transgenic expression and activation of PGC-1 α protect dopaminergic neurons in the MPTP mouse model of Parkinsons disease. *Cell Mol Life Sci.* 2012;69: 1153–65.
49. Yi X, Guo W, Shi Q, Yang Y, Zhang W, Chen X, et al. SIRT3-dependent mitochondrial dynamics remodeling contributes to oxidative stress-induced melanocyte degeneration in vitiligo. *Theranostics.* 2019;9:1614–33.
50. Dai SH, Chen T, Wang YH, Zhu J, Luo P, Rao W, et al. Sirt3 protects cortical neurons against oxidative stress via regulating mitochondrial Ca²⁺ and mitochondrial biogenesis. *Int J Mol Sci.* 2014;15:14591–609.
51. Yang X, Geng K, Zhang J, Zhang Y, Shao J, Xia W. Sirt3 Mediates the inhibitory effect of adjuvins on astrocyte activation and glial scar formation following ischemic stroke. *Front Pharmacol.* 2017. <https://doi.org/10.3389/fphar.2017.00943>.
52. Pi H, et al. SIRT3-SOD2-mROS-dependent autophagy in cadmium-induced hepatotoxicity and salvage by melatonin. *Autophagy.* 2015;11(7):1037–51.
53. Zhai M, et al. Melatonin ameliorates myocardial ischemia reperfusion injury through SIRT3-dependent regulation of oxidative stress and apoptosis. *J Pineal Res.* 2017;63(2):e12419.
54. Sharabi K, Lin H, Tavares CDJ, Dominy JE, Camporez JP, Perry RJ, et al. Selective chemical inhibition of PGC-1 α gluconeogenic activity ameliorates type 2 diabetes. *Cell.* 2017;169:148-160.e15.
55. Lim J, Choi HS, Choi HJ. Estrogen-related receptor gamma regulates dopaminergic neuronal phenotype by activating GSK3 β /NFAT signaling in SH-SY5Y cells. *J Neurochem.* 2015;133:544–57.

Publisher's Note Springer Nature remains neutral with regard to jurisdictional claims in published maps and institutional affiliations.

Springer Nature or its licensor (e.g. a society or other partner) holds exclusive rights to this article under a publishing agreement with the author(s) or other rightsholder(s); author self-archiving of the accepted manuscript version of this article is solely governed by the terms of such publishing agreement and applicable law.